Electromagnetic analysis of ITER equatorial Wide Angle Viewing System (WAVS) in-vessel components

S. Garitta, C. Portafaix, L. Letellier, C. Guillon, F. Le Guern, P. Testoni, J. Guirao, M. Kocan

Version of Record: https://www.sciencedirect.com/science/article/pii/S0920379621002477
Manuscript_74628e2c2824849d7f8fe02db459fc21

Electromagnetic Analysis of ITER equatorial Wide Angle Viewing System (WAVS) in-Vessel Components

S. Garitta[1], C. Portafaix[1], L. Letellier[1], C. Guillon[1], F. Le Guern[2], P. Testoni[2], J. Guirao[3], M. Kocan[3]

[1]*CEA, IRFM, F-13108 Saint-Paul-Lez-Durance, France*
[2]*F4E, Josep Pla 2, Torres Diagonal Litoral B3, 08019 Barcelona, Spain*
[3]*ITER Organization, Route de Vinon sur Verdon, CS 90 046, 13067 Saint-Paul-lez-Durance, France*

In the framework of ITER diagnostics, the visible and infrared equatorial Wide Angle Viewing System (WAVS, referenced as 55.G1.C0 in ITER Plant Breakdown Structure) plays a key role. Indeed, this system is devoted to monitor the surface temperature of the plasma facing components by infrared thermography and to image the edge plasma emission in the visible range. As a consequence, it is mandatory to verify that WAVS components are able to withstand all the foreseen loads and load combinations. This paper is dedicated to present the methods and results of electromagnetic (EM) and Transient Structural (TS) analyses for determining the loads due to Eddy Currents and the associated stresses and displacements in the in-vessel components of WAVS at its Preliminary Design Review (PDR) stage.

Specifically, the analysed WAVS in-vessel components comprise First Mirror Units, shutters and Hot Dog Legs of the EPP#12 (Equatorial Port Plug). The selected EM loads derive from the IO-assumed worst EM scenario for EPP#12 (specifically a plasma exponential major disruption).

Given the variation maps of the global magnetic field in the regions of interest during the transient, the EM loads have been estimated using a local 3D EM model of the WAVS components by means of the ANSYS Electromagnetics Suite v.19.2, employing the tool ANSYS Maxwell. Successively, the obtained results have been used as inputs to the corresponding TS analyses (carried out using ANSYS Workbench v.19.2). Therefore, the related outcomes can be combined with the set of all other structural studies (i.e. thermal and seismic analyses) to assess the overall mechanical behaviour of the components under study for the WAVS PDR level. Moreover, the results obtained have shown how EM loads are often design driving loads for the WAVS components.

Keywords: ITER, 55.G1.C0, WAVS, electromagnetics, eddy currents, disruption, EM loads, Transient Structural

1. Introduction

The visible and infrared equatorial Wide Angle Viewing System (WAVS, referenced as 55.G1.C0 in ITER Plant Breakdown Structure) is one of the key diagnostics in ITER, being devoted to machine protection, plasma control and physics analysis. It comprises 15 Lines of Sights (LoSs) to be installed in four equatorial ports (#03, #09, #12 and #17), foreseen to allow the monitoring of the surface temperature of the main in-vessel components and imaging the edge plasma emission in the visible range. [1]

For the in-vessel Components PDR (Preliminary Design Review), the three lines of sight of the WAVS design integrated within the Diagnostic Shield Module #1 (DSM#1) of the Equatorial Port #12 (EP#12) have been developed and taken into account. The reason why EP#12 has been chosen is that this port has been selected as a first plasma port. The first plasma phase corresponds to the very first starting of the machine and, as a matter of fact, the complete design of the two first plasma in-port components, which include equatorial ports 11 and 12, are now past the final design reviews and will soon be in manufacturing, as indicated in [2].

Within the framework of the activities foreseen for the WAVS PDR level, a research campaign has been carried out at CEA Cadarache, in cooperation with ITER Organization and Fusion for Energy (F4E), to investigate the Electromagnetic (EM) loads the in-vessel components shall withstand during a representative plasma disruption. Moreover, these results have been used as input to the relative Transient Structural (TS) calculations, which have been included in the assessment of the overall mechanical behaviour of the components under study.

The research campaign has been carried out using local 3D EM models of the WAVS components by means of the ANSYS Electromagnetics Suite v.19.2, employing the tool ANSYS Maxwell. Successively, the corresponding TS analyses have been carried out in ANSYS Workbench v.19.2.

Analysis models, assumptions, loads and boundary conditions are herein reported and critically discussed, together with the main results obtained.

2. WAVS overview

The main features of the WAVS system are described in [1] and [3], developments of earlier concepts reported in [4] and [5]. In the EPP#12 three "drawers" are implemented. The WAVS is embedded in the "drawer" on the right side when looking the ex-vessel part from the plasma point of view. Fig.1 (upper part) shows a cutaway view of DSM#1 in EPP#12. Red pyramids and cylinders represent the optical beams for the three LoSs along the DSM#1: the bottom LoS

*Corresponding author: silvia.garitta@cea.fr

(Divertor's view) collects photons coming from the divertor, while both above LoSs (tangential views) collect photons coming from the outer & inner blanket first walls.

Each LoS is composed of two mirrors units in the port plug, which is under vacuum conditions (Fig.1, lower part):

- First Mirror Unit (FMU): being the closest to the plasma, it is the most exposed part of the system, it is actively water cooled and has a shutter to occult the optical path and protect the optical surfaces when needed. Fig.2 shows a vertical cut of the FMU with the photon beams focused through a pupil drilled in the actively cooled part (the so called "tent") covering the two first mirrors. Fig.3 depicts the shutter version that has been analysed in this paper (this component has undergone many changes and developments), with a cut view on the right to highlight the internal bellows and (helicoidal) water channels.

- Hot Dog Leg mirrors unit (HDL): it is the second part of the optical chain of optical components, transmitting photons from the FMU to the ex-vessel part, and it works as a periscope to minimize neutrons direct radial streaming through the DSM#1. The common structure supporting both HDL mirrors is equipped with two mechanical tents protecting the mirrors against the Remote Handling (RH) operations to install them inside the DSM#1. Furthermore, at this stage, no cooling is foreseen for this component (the nuclear volumetric heating exponentially decreases with the distance from the plasma). Fig.4 and Fig.5 illustrate the HDL Left and Divertor Views, respectively, also highlighting their RH elements (that are the parts necessary to connect the RH tools during maintenance in the hot cells).

Both tangential LoSs are very similar in their design. The position of the mirrors changes slightly but the optical elements remain the same at first order.

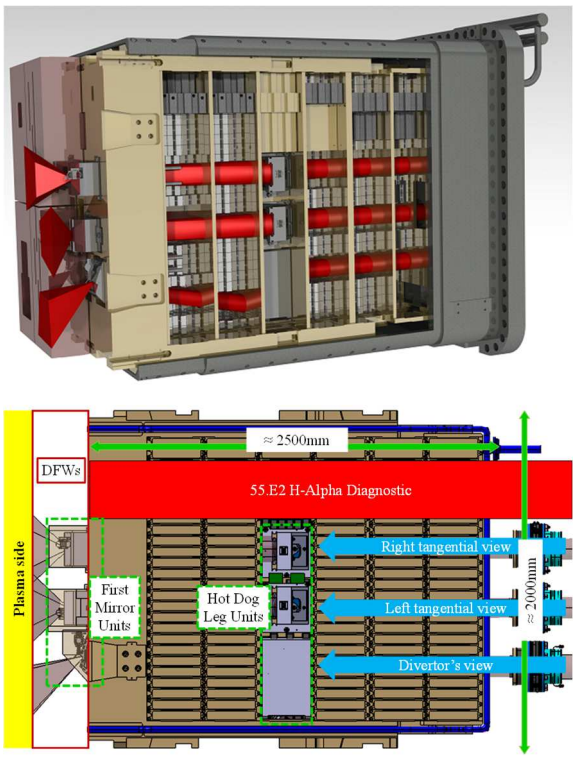

Fig.1. WAVS inside DSM#1 in EPP#12

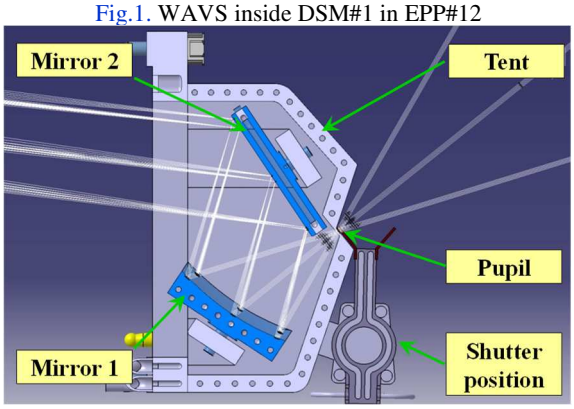

Fig.2. FMU's vertical cut (plasma is on the right).

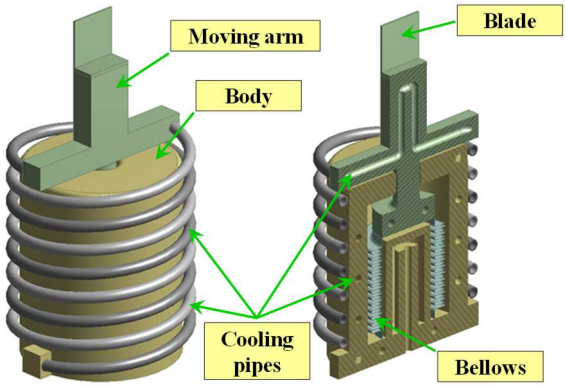

Fig.3. FMU's shutter (analysed geometry).

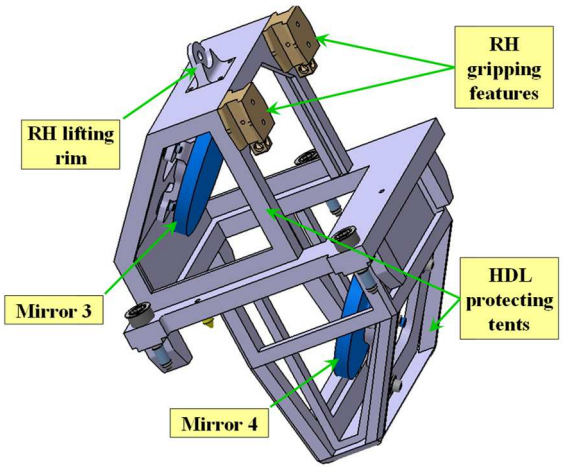

Fig.4. HDL Left View.

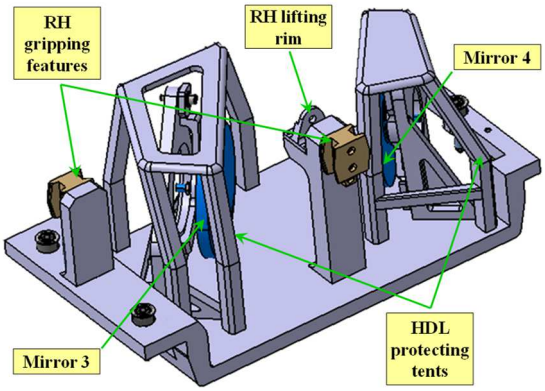

Fig.5. HDL Divertor View.

3. Evaluation of the EM scenario

The main electromagnetic loads will occur in ITER due to transient events. These loads may be significant in the case of the diagnostic systems placed inside port plugs and need to be carefully evaluated. At PDR stage, the EM loads on the DSM#1 are provided for the assumed worst EM event for Equatorial Port Plug in category III: MD DW exp16ms with thermal quench of 0.5ms. [6] [7] Specifically, according to the ITER System Load Specification [8], the ITER loading conditions are categorized into four classes, based on the expectation of occurrence. Among them, category III represents the "Unlikely Loading Conditions". Moreover, according to [9], the worst case for the generic EPP assembly is a Major Disruption (MD) of a 15 MA plasma current moving downward (DW) and decaying exponentially to zero within 16 milliseconds.

Given the maps of evolution of the magnetic field in the region of interest, the EM loads can be estimated using a local EM model of the WAVS components. The rate of change of the fields and the fields during this event can be used to evaluate the Eddy Currents and the EM loads.

The diagnostic generic EM Finite Element (FE) model described in [7] and depicted in Fig.6 and Fig.7 consists of a complete 20º ITER sector that implements a modular DSM inside the EPP. In the bottom part of Fig.7, there is the detail of the DSM#1 along with a representation of magnetic field (B field) in the toroidal direction (B_Y) at a specific time, as an example of the acquired analysis outputs. Once the component to be analysed is chosen, a corresponding box-shaped region inside the DSM space is selected, focussing the attention on how the three components of the magnetic field evolve in time there during the considered MD event.

Given these maps of evolution of the magnetic field in the regions of interest, the EM loads have been estimated using a local EM model of the WAVS components at the PDR stage. Specifically, the EM loads to be given as inputs to the EM characterisation of the ITER WAVS components are supposed to be uniform in each considered region of space, while changing in time during the transient event. Therefore, representative magnetic field values have been chosen for each analysed component.

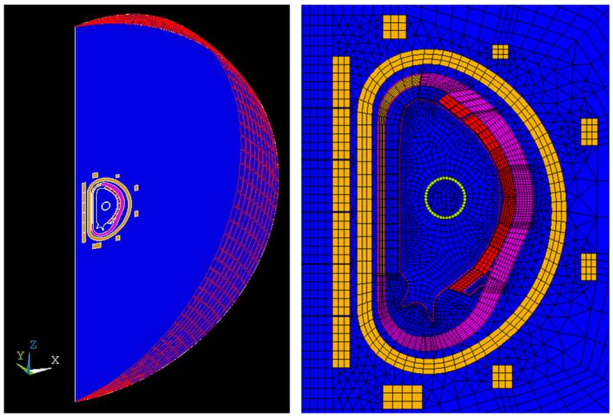

Fig.6. ITER sector EM FE model (vacuum domain included).

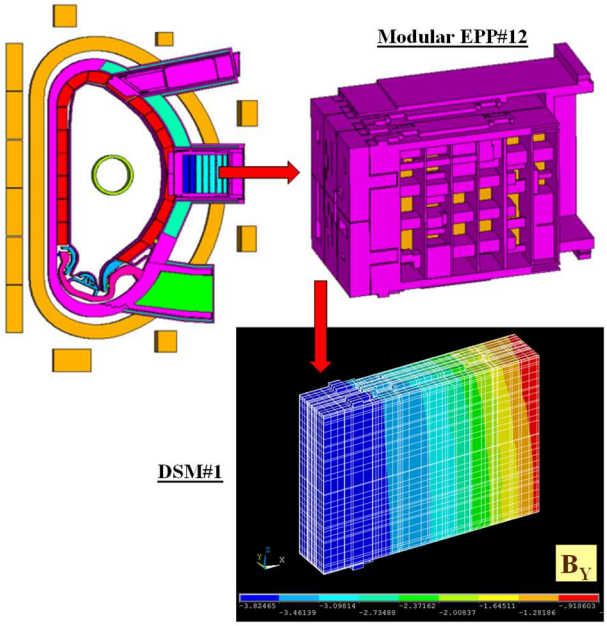

Fig.7. ITER sector EM FE model - integrated EPP#12.

This local approach is compliant with the WAVS in-vessel SLS (System Load Specification, [6]) and it has been chosen as a compromise to allow more efficient

iterations between analysis results and components development. However, being a rather simplified method, it will not be used for the next WAVS developing phases, giving way to more global and specific models (such as calculations with the components incorporated inside the whole ITER EM FE sector).

Once selecting the B field variations to be employed, they have been imposed as loads thanks to the following procedure. If a current density J_0 flows in a stationary spherical shell with a thickness decreasing with cosinusoidal law, the equivalent and uniform magnetic field B_0 that is obtained in the central region of the current sphere results in:

$$B_0 = \frac{2}{3} \cdot \mu_0 \cdot J_0 \qquad (1)$$

with $\mu_0 = 4\pi \cdot 10^{-7}$ N/A^2 (vacuum permeability). [10]

If $B_i(t)$ is the requested time-varying magnetic field (in the i direction), S_i the cross section surface of the sphere (highlighted in Fig.8) and $s_{i,0}$ its equatorial thickness, the current that needs to be imposed on S_i is:

$$I_i(t) = \frac{3 \cdot B_i(t) \cdot S_i}{2 \cdot \mu_0 \cdot s_{i,0}} \qquad (2)$$

Fig.8 illustrates the three spheres and the surfaces S_i in which the corresponding currents $I_i(t)$ (derived from Eq.(2) and an example of which is shown in Fig.9) are applied.

Moreover, each EM calculation also comprises a superimposed vacuum region with a 150% padding.

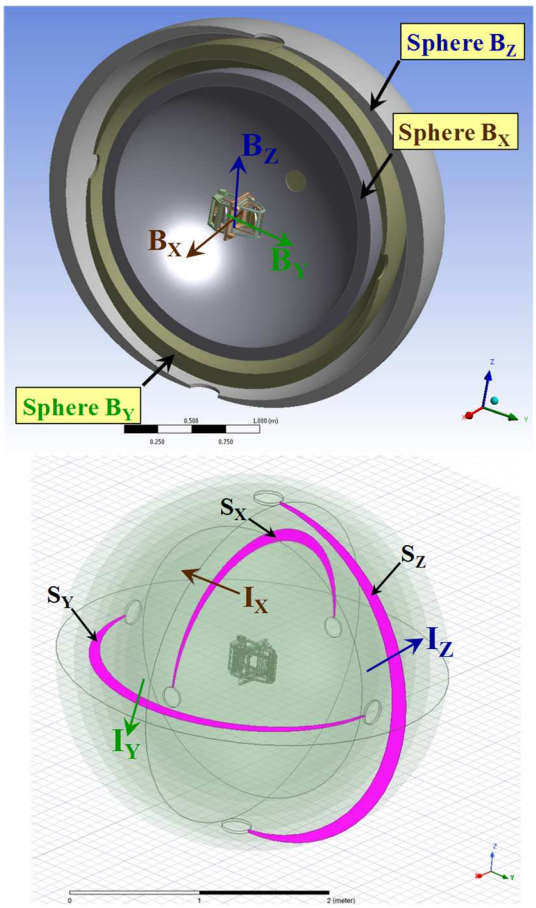

Fig.8. ITER WAVS components EM analysis geometrical domain

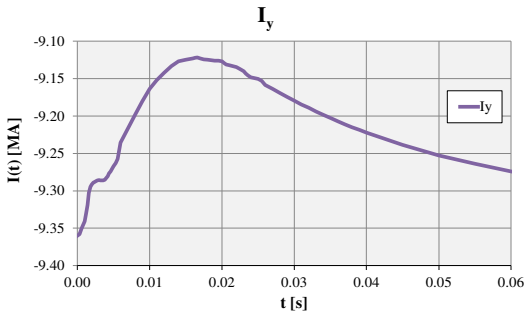

Fig.9. ITER WAVS components EM analysis representative imposed current.

In summary, the performed analysis type is a 3D transient EM calculation with time-varying currents imposed to three spheres as inputs. These excitations create an internal region with a space-uniform magnetic field that, being variable in time, induces Eddy Currents inside the components. These currents produce an interaction with the magnetic field resulting in forces and torques. Additionally, this methodology allows to obtain results which are detailed enough to be used as inputs to the corresponding TS analyses.

4. Verification of the employed procedure

Naturally, a benchmark of these EM and TS procedures has been performed to validate the employed method. First, a very simple magnetostatic analysis

containing a single sphere with a conductive solid has been carried out, verifying that the wanted uniform magnetic field is actually obtained.

Successively, a magnetic transient analysis has been set up modelling two concentric spherical shells along with a stainless steel circular coil (Fig.10, upper part). The outer shell (Sphere B_Z) is interested by a constant current to produce a time-constant magnetic field oriented with the z axis. The inner one (Sphere B_X), on the other hand, is oriented with the x axis and it is supposed to induce an exponential time-varying magnetic field. As a result of the varying magnetic field, a current *I(t)* is induced inside the circular coil, whose theoretical formulation derives from:

$$R \cdot I(t) + L\frac{dI(t)}{dt} = -\frac{d\Phi(B_X)}{dt} \quad (3)$$

with *R* the electrical resistance, *L* the inductance of the coil and $\Phi(B_X)$ the magnetic flux due to the B field in the x direction [10]. These theoretical results have been compared with the induced current evolution evaluated with Maxwell, finding a good correspondence (Fig.10, lower part), with an average variation less than 3% (equal to 2.9% when the maximum current value is reached). An analogous average variation has been found between theoretical and Maxwell results comparing the torque M_{Y0} of the coil around the y axis (due to the Lorentz forces produced by the interaction between the current in the coil and B_Z).

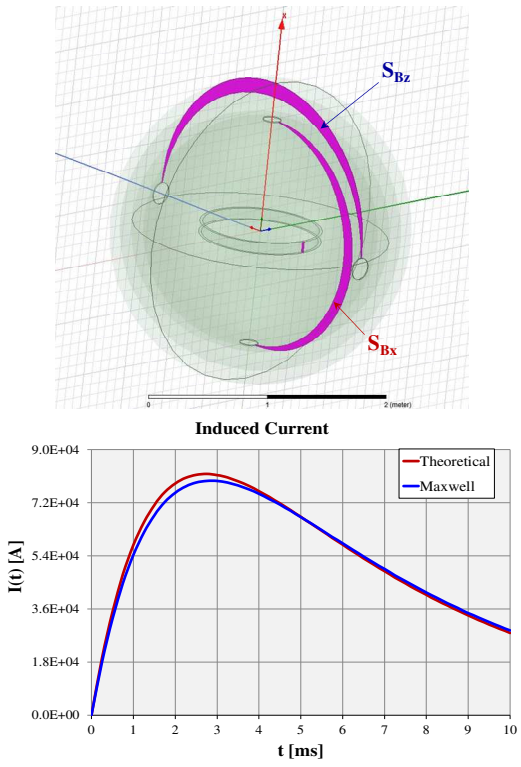

Fig.10. Benchmark EM calculation domain and results

Moreover, this EM analysis has been employed as input for a TS analysis on the model, as shown in the upper part of Fig.11. Specifically, in this image are depicted both the obtained EM Body Force Density imported as load as well as the two springs chosen as mechanical constraint and placed in two diametrically opposite points of the rigid coil. As shown in the lower part Fig.11, a good correspondence (with an average variation less than 8%, equal to 3.5% when the maximum torque value is reached) has been also found between the ANSYS results and the theoretical formulation for the spring elongation deriving from the equation of motion:

$$J \cdot \ddot{\phi} = \sum M_i = M_{Y0} - 2 \cdot F_S \cdot r \quad (4)$$

with *J* as the coil moment of inertia around the y axis, ϕ the rotational angle, F_S the spring force and *r* the average coil radius.

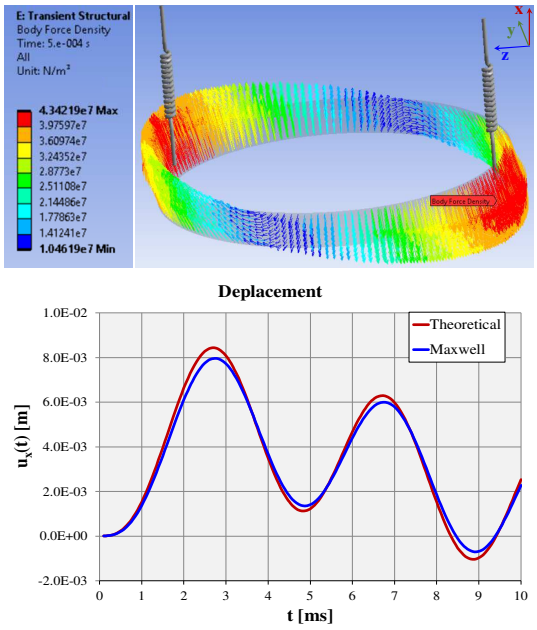

Fig.11. Benchmark TS calculation domain and results

5. WAVS components EM analysis campaign

Small geometrical simplifications (i.e. deleting pins, screws and bolts, filling small holes and gaps) have been carried out to facilitate EM calculations without influencing the quality of the results. In addition, since the shutter is characterised by a very complex structure, its behaviour has been evaluated separately from the corresponding FMU component. Moreover, the shutter has been also appreciably simplified in order to allow its calculation, setting-up a heavy but still viable and manageable model, leaving a more detailed representation to future studies.

As far as the employed materials are concerned, their properties have been selected according to [11], [12] and [13]. All parts of the HDL components are considered to be Stainless Steel SS316L(N)-IG, as well as the FMU components, except for FMU mirrors, which are in copper-chromium-zirconium alloy (CuCrZr). Moreover, also the overall shutter is in stainless steel, with only the blade in CuCrZr. Finally, copper conductivity has been used as far as the spheres are concerned, even though the spheres response has no impact on the analyses results since Eddy Currents have not been considered in them.

Table 1 lists all materials properties used in the analysis campaign, which have been evaluated at 100°C, except for the electrical conductivity, that refers to 70°C (conservative hypothesis).

stainless steel - SS316L(N)-IG	
Electrical conductivity - σ [S m^{-1}]	$1.3 \cdot 10^6$
Relative permeability - μ_r	1
Mass density - ρ [kg m^{-3}]	7 899
Young's Modulus - E [Pa]	$193 \cdot 10^9$
Poisson's Ratio - υ	0.3
copper-chromium-zirconium alloy - CuCrZr-IG	
Electrical conductivity - σ [S m^{-1}]	$4.0 \cdot 10^7$
Relative permeability - μ_r	1
Mass density - ρ [kg m^{-3}]	8 900
Young's Modulus - E [Pa]	$127 \cdot 10^9$
Poisson's Ratio - υ	0.33

Table 1. Materials employed properties.

An element length based refining has been adopted for the EM model mesh, setting the value of maximum element length inside each component (according to the results of a mesh independency sensitivity analysis). Table 2 summarises the global mesh number of elements (tetrahedrons) for each carried out EM calculation. Specifically, the table highlights how many of the overall elements have been devoted to the actual WAVS component with respect of the global domain (which also contains the three spheres and the cubic vacuum region). Furthermore, the denser mesh for the shutter is due to its much smaller structures than the ones relating to the other WAVS components.

N° of elements	**WAVS component**	**Global domain**
HDL Left View	183 115	430 711
FMU Left View	337 422	690 574
HDL Right View	162 283	405 063
HDL Divertor View	279 187	553 980
FMU Divertor View	437 970	964 362
Shutter Tangential View	793 404	1 280 683
Shutter Divertor View	800 334	1 299 146

Table 2. ITER WAVS EM calculations mesh summary.

The performed type of analysis is a 3D transient EM calculation. The analysis inputs are time-varying current values imposed to the three spheres that surround the selected ITER WAVS component (details in paragraph 3). These currents create an area in the central part of the spheres in which the magnetic field is constant in the space domain but variable in time.

During the transient, Eddy Currents are induced inside the components, since they experience time-varying magnetic fields. These currents produce an interaction with the magnetic field resulting in forces and torques. Additionally, the results obtained from the EM calculations have been used as inputs to the relative TS analyses.

The first 50 ms of the ITER MD transient have been analysed, specifically setting a time step of 0.2 ms for the first 30 ms and of 2 ms for the last 20 ms (consistently with the input ITER MD event calculation). Successively, the Body Force Densities obtained from these EM analyses have been directly imported (through Workbench connection) and used as load for the TS steps.

Considering the HDL Left View as an example, Fig.12 and Fig.13 show the mesh for the EM calculation, Fig.14 illustrates the torques along the three main directions during the transient, while Fig.15 gives a representation of the Eddy Currents inside the component at the time when the maximum torque is reached.

Furthermore, Fig.16 highlights the imposed Boundary Conditions (BCs) (blocking displacements in positions from A to E to take into account the presence of bolts and pins) as well as the adopted Hexahedral Dominant mesh for the TS step. Fig.17 gives the maximum equivalent Von Mises stress time distribution. In addition, since the location of the maximum equivalent stress changes with different time steps, Fig.18 illustrates the location of all the maximum stress values over time. Finally, the total deformation space distribution at the peak instant of time is depicted in Fig.19.

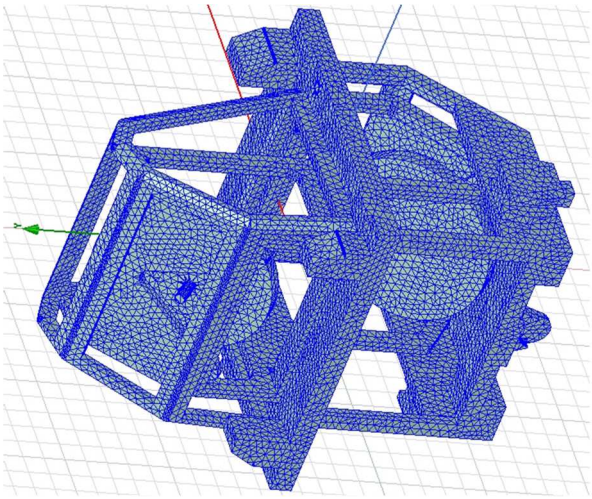

Fig.12. HDL Left View EM calculation - Left View mesh.

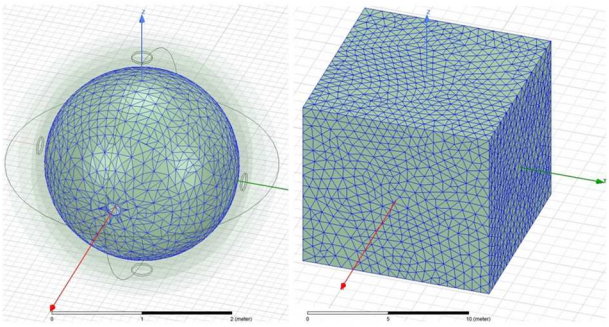

Fig.13. HDL Left View EM calculation - Sphere Bx and vacuum region mesh.

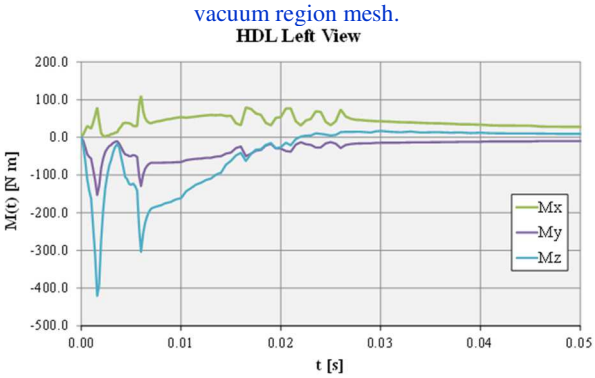

Fig.14. HDL Left View EM calculation torques

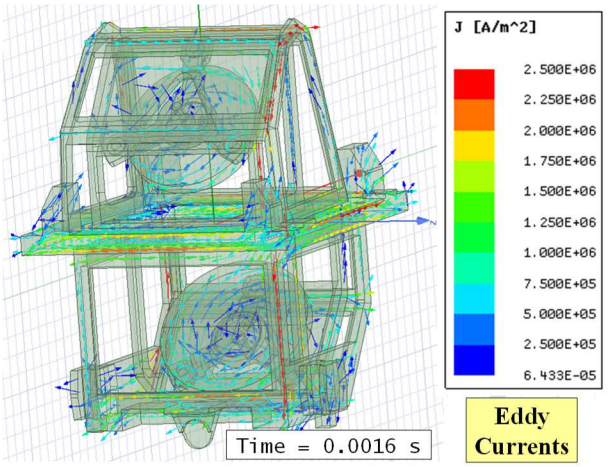

Fig.15. HDL Left View EM calculation Eddy Currents

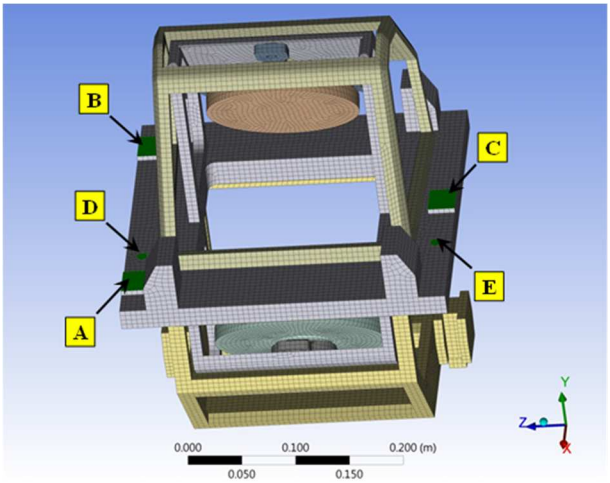

Fig.16. HDL Left View TS calculation BCs and mesh

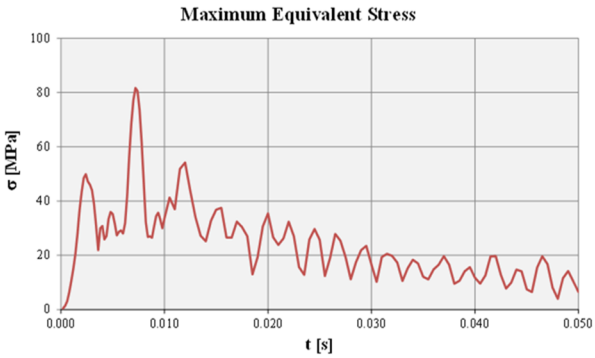

Fig.17. HDL Left View maximum Von Mises equivalent stress

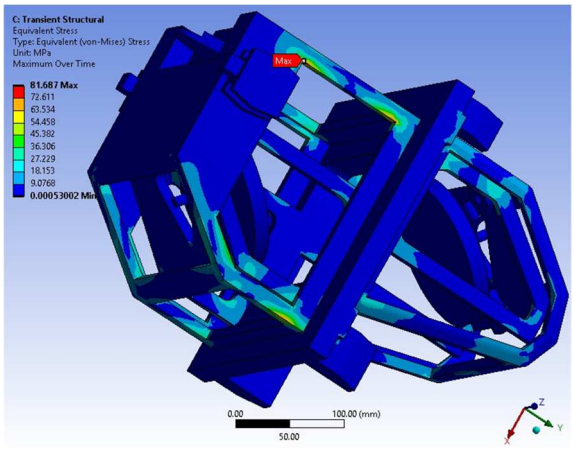

Fig.18. HDL Left View maximum equivalent stress over time

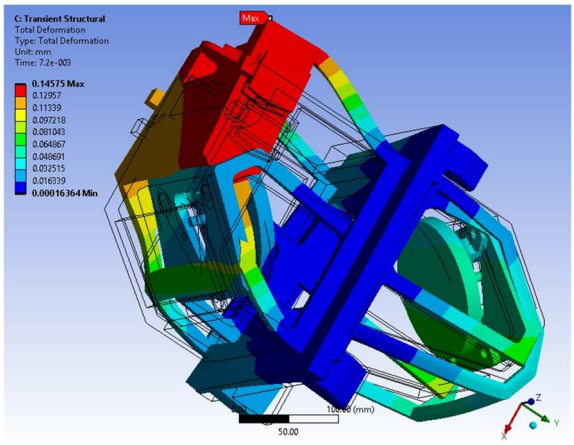

Fig.19. HDL Left View total deformation distribution

The main results in terms of torques, stress and displacement of the EM-TS calculations of ITER WAVS in-vessel components are summarised in Table 3 and Table 4 (for the shutter, the TS calculation of only the Tangential View has been carried out).

These outcomes of the TS calculations have been used as part of the assessment of the overall mechanical behaviour of the WAVS components at the PDR level, as extensively reported in [14]. This global study has shown how EM loads always give a significant contribution in the overall evaluated mechanical stress, often resulting in design driving loads.

EM calculations	$M_{X, MAX}$ [N m]	$M_{Y, MAX}$ [N m]	$M_{Z, MAX}$ [N m]
HDL Left View	110.0	-152.7	-420.5
FMU Left View	1193.3	-323.7	-760.7
HDL Right View	227.2	27.9	337.7
HDL Divertor View	100.0	-103.4	-380.2
FMU Divertor View	849.1	-284.5	-797.7
Shutter Tangential View	137.2	-19.0	-32.4
Shutter Divertor View	59.0	-12.3	-14.5

Table 3. Torques results summary of the EM calculations.

TS calculations	σ_{MAX} [MPa]	U_{MAX} [mm]
HDL Left View	81.7	0.15
FMU Left View	130.5	0.18
HDL Right View	78.3	0.29
HDL Divertor View	79.4	0.32
FMU Divertor View	200.0	0.33
Shutter Tangential View	141.2	2.60

Table 4. Stress (Von Mises) and displacement summary of the TS calculations.

6. Conclusions

In the framework of the ITER diagnostics, the visible and infrared equatorial Wide Angle Viewing System (WAVS) plays a key role, being devoted to monitor the surface temperature of the plasma facing components by infrared thermography and to image the edge plasma emission in the visible range.

The performed analysis campaign has been dedicated to determine the loads due to Eddy Currents in the WAVS in-vessel components at its Preliminary Design Review stage.

Given the maps of evolution of the global magnetic field in the regions of interest during the EM event for EPP in category III (MD DW exp16ms with thermal quench of 0.5ms), the EM loads due to Eddy Currents have been estimated using local 3D EM models of the components by means of ANSYS Maxwell v.19.2.

Successively, the obtained results of the Electromagnetic calculations have been used as inputs to the relative Transient Structural analyses (carried out by means of ANSYS Workbench v.19.2).

Moreover, a preliminary benchmark of these EM and TS procedures has been performed to validate the method.

Finally, the TS outcomes have been used as part of the assessment of the overall mechanical behaviour of the components under study for the WAVS PDR level, showing how EM loads are often design driving loads for the WAVS components.

Acknowledgments

This work was performed with Fusion for Energy and their partial financial support in the framework of the contract F4E-FPA-407. The views and opinions expressed herein do not necessarily reflect those of Fusion for Energy nor those of the ITER Organization.

References

[1] C. Guillon et al., *F4E-FPA-407 SG04 D10 CD09 System Design Description of PBS 55.G1.C0 Port-Plug components v1.5*, private communication, F4E (2FPKP6 v3.0) and ITER (2DMZ4D v1.0) IDM report, 2019

[2] B. Bigot, *ITER assembly phase: Progress toward first plasma*, Fusion Eng. Des. 164 (2021) 112207

[3] L. Letellier et al., *System level design of the ITER equatorial visible/infrared wide angle viewing system*, Fusion Eng. Des. 123 (2017) 650–653

[4] R. Reichle, et al., *Concept development for the ITER equatorial port visible/infrared wide angle viewing system*, Rev. Sci. Instrum. 83 (2012) 10E520

[5] S. Salasca, et al., *The ITER equatorial Visible/IR wide angle viewing system: status of design and R&D*, Fusion Eng. Des. 96–97 (2015) 932–937.

[6] M. Kocan et al., *Load Specification for Visible/IR Wide Angle Viewing System in Equatorial Port Plug of EP12*, private communication, ITER IDM report (BJHNF8 v3.1), 2019

[7] J. Guirao et al., *EM_Analysis_55.Eq#11/12*, private communication, ITER IDM report (URBGMU v1.1), 2017

[8] G. Sannazzaro, *Load Specifications (LS)*, private communication, ITER IDM report (222QGL v6.2), 2017

[9] J. Zhai et al., *Development of load specifications for the design of ITER diagnostic system and port integration*, Fusion Eng. Des. 123 (2017) 743–748

[10] E. Durand, *Magnétostatique*, Masson et C.ie editeurs, 1968

[11] V. Barabash et al., *Appendix A, Materials Design Limit Data*, private communication, ITER IDM report (222RLN v3.3), 2013

[12] V. Barabash et al., *AA04-3201 316L (N)-IG Stainless Steel - Electrical Resistivity*, private communication, ITER IDM report (222W3R v1.0), 2008

[13] V. Barabash et al., *CuCrZr - Electrical Resistivity*, private communication, ITER IDM report (2232UB v1.1), 2009

[14] N. Lefevre et al., 55.G1.C0_Structural Integrity Report(s), private communication, F4E (2GCWVT) and ITER (2E9924 v1.1) IDM report, 2019